

Evolution and fluctuations of chiral chemical potential in heavy ion collisions

Vladimir Kovalenko *

*Saint Petersburg State University,
7/9 Universitetskaya Nab., St. Petersburg 199034, Russia
v.kovalenko@spbu.ru*

The possible appearance of the effects of local parity breaking in the QCD medium formed in heavy ion collisions due to violation of chiral symmetry can be quantified by corresponding chiral chemical potential μ_5 . The experimental observables sensitive to the effects of local parity violation in strong interaction include search for polarisation splitting of the ρ_0 and ω_0 mesons via angular dependence of spectral functions in their decay to leptons. In this paper we study the space-time evolution and fluctuations of μ_5 using relativistic hydrodynamics and estimate their effect on the light vector meson polarization splitting in Pb-Pb collisions at LHC energy.

Keywords: local parity violation; chiral imbalance; chiral chemical potential; relativistic hydrodynamics

PACS numbers: 11.30.Er, 11.30.Rd, 24.10.Nz, 13.20.-v

1. Introduction

The strong interaction, as it is well known, obey the global spatial (P) parity conservation. So far, no evidence has been found for violation of P- and CP-symmetries in strong interactions. However, quantum chromodynamics (QCD) does not forbid the local parity symmetry breaking due to large topological fluctuations at high temperature with dynamic generation of nontrivial topological charge configurations. A necessary condition for observing these effects is a sufficiently large space dimension and a long lifetime of a hot drop of QCD medium, which is available in central nuclear-nuclear collisions at the LHC [1–3].

In the presence of a hot medium in the state of deconfinement, formed in heavy ion collisions, the modification of the properties of hadrons is possible. They can arise due to the inhomogeneity of the medium, as well as due to such non-perturbative effects as, for example, instantons [4]. In the perturbative calculations, the amplitudes of transitions between different degenerate vacua, connected by topologically non-trivial gauge transformations, are equal to zero in any order of the perturbation theory. However, they can afford for nonperturbative phenomena, known as sphaleron transition [5–7], happening through a potential barrier sepa-

*Corresponding author.

rating topologically nonequivalent vacua. Such configurations can be excited in the collision of heavy ions, or initially exist in them [1, 2].

So it can be assumed that parity-violating bubbles can arise in a collision of relativistic nuclei in a finite volume, causing the effect of a local parity nonconservation. The behavior of the topological charge of the gauge fields existing in a fireball for a long time, in statistical approach, can be described in terms of topological chemical potential (μ_θ). Due to the partial nonconservation of the axial current in QCD, in the approximation of low fermion masses, it is possible to relate the topological charge to the value of the chiral imbalance, which is defined as the average difference between the number of right and left quarks in a fireball after heavy ion collisions at high energy [8]. Thus, chiral imbalance can lead to the formation of local parity violation (LPB) in a quark-hadron medium with local thermodynamic equilibrium characterized by an axial chemical potential [9]. In this case, a connection arises between the topological (μ_θ) and axial (μ_5) chemical potentials:

$$\mu_5 = \frac{1}{N_f} \mu_\theta, \quad (1)$$

where N_f is a number of flavors.

The effect of local parity nonconservation in strong interactions can be experimentally searched for using local observables sensitive to the processes at hadron space scale, which are not canceled out after the summation over the whole medium.

It was shown in [10–13] that this effect can be verified experimentally by analyzing the yields of dilepton pairs in the region of small invariant masses in heavy ion collisions. This will require simultaneous scanning of both the invariant mass (m_{ll}) and the expansion angle (θ_A) of leptons from the decays of light vector mesons. In the case of a nonzero axial chemical potential, a polarization splitting of the spectral functions of ρ and ω mesons occurs in a part of the phase space, with the formation of a characteristic two-peak structure.

Later, it was shown [14] that if the radiative corrections are taken into account, then the presence of the axial chemical potential leads not only to the splitting of the masses of the left and right polarizations of vector mesons, but also to their general shift towards an increase. These effects depend both on the value of the axial chemical potential μ_5 and on the momentum of the vector meson (k).

Because the polarization mass splitting depends on the axial chemical potential μ_5 , the experimentally measured picture would depend also on the fluctuations of μ_5 . There is a risk that in case of sufficiently large fluctuations the splitting would smear out and become hard to detect. So the main purpose of the paper is to investigate the evolution of the axial charge density during heavy ion collision from the initial stages to freeze-out and to estimate its fluctuations induced by this evolution.

We should add that other ways of observation of parity nonconservation effects in heavy ion collisions are possible. In the presence of the large magnetic field,

which is characterized by semi-central and peripheral ion collisions, the so-called chiral magnetic effect (CME) can happen [9, 15]. It was measured at RHIC and LHC [16–18] and a CME-like signal was found. However, other backgrounds, like a local charge conservation, play a comparable role [19]. Nevertheless, the comparison of the experimental results with modeling [20] showed the best agreement is achieved for the μ_5 above 300 MeV.

The evolution of the axial charge in the QCD medium is modeled using Anomalous-Viscous Fluid Dynamics (AVFD) framework [21] for studying the signatures of chiral magnetic effect in relativistic nuclear collisions [22, 23] (see also review papers [24–26]). The main attention is devoted to the calculation of chiral magnetic effect in presence of magnetic field in non-central heavy-ion collisions. In the present work we focus on modeling parity-violating effects [10–13] relevant also for central nucleus-nucleus collisions.

We should note that apart from the vector meson parity mass splitting [10–13] there are other proposals, also suitable for central heavy-ion collisions, including the search for decays of a scalar charged a_0 meson into a photon and a charged pion or into three charged pions [27–32], study the relative rate of π meson decay by muon-neutrino and electron-neutrino channels [30], search for possible asymmetry of the photon polarization [33].

2. Methods

The simulation of the evolution of the QCD medium produced in heavy ion collisions at LHC energy has been performed using relativistic hydrodynamics. A commonly-used package MUSIC [34–37], 3+1D relativistic second-order viscous hydrodynamics for heavy ion collisions, was used. In this studies, for simplicity, boost-invariant 2+1D version was taken. Lattice hotQCD equation of state (EOS) was used, and no dependence in EOS on μ_5 were assumed. The viscosity over entropy density parameter is set as $\eta/s = 0.08$.

The initial energy density distributions were generated using the Glauber Monte Carlo sampler [38, 39] with the initial entropy density deposited at wounded nucleon positions. Central Pb-Pb collisions at 5.02 TeV (with impact parameter $0 < b < 2$ fm) were considered.

The initial axial charge [40, 41] densities were set up as negative and positive isolated areas in the transverse plane with radius of 2.1 fm with the constant ρ_5 inside them and zero total axial charge (see Figure 1). In the case of ideal evolution, the net axial current evolves according to the following equation [42]:

$$\partial_\mu J_5^\mu = -\frac{N_c Q_f^2}{2\pi^2} E \cdot B. \quad (2)$$

In case of central collisions the magnetic field is small, so we put electromagnetic fields B, E as zero. With this assumption the equation (2) becomes the continuity equation.

In order to take into account the viscous dissipative effects and the damping of axial charge due to gluon topological fluctuations [42], the Anomalous-Viscous Fluid Dynamics (AVFD) framework [21, 43] was applied. In this framework it is possible to consider the 2+1D hydrodynamic history of the QCD fluid, modeled with MUSIC [34–37], as a background and to perform the 2nd order evolution of the left-handed ($\chi = -1$ and right-handed $\chi = 1$) fermion currents:

$$\begin{aligned}
\hat{D}_\mu J_{\chi,f}^\mu &= \chi \frac{N_c Q_f^2}{4\pi^2} E_\mu B^\mu \\
J_{\chi,f}^\mu &= n_{\chi,f} u^\mu + \nu_{\chi,f}^\mu + \chi \frac{N_c Q_f}{4\pi^2} \mu_{\chi,f} B^\mu \\
\Delta^\mu \hat{d}(\nu_{\chi,f}^\nu) &= -\frac{1}{\tau_r} \left[\left(\nu_{\chi,f}^\mu \right) - \left(\nu_{\chi,f}^\mu \right)_{NS} \right] \\
\left(\nu_{\chi,f}^\mu \right)_{NS} &= \frac{\sigma}{2} T \Delta^{\mu\nu} \partial_\nu \left(\frac{\mu_{\chi,f}}{T} \right) + \frac{\sigma}{2} Q_f E^\mu
\end{aligned} \tag{3}$$

The dissipative effect is guided by the diffusion coefficient σ and relaxation time τ_r . Again, we put magnetic field as zero.

During the hydrodynamic evolution, there exist random topological fluctuations of the gluon fields that can influence the axial current evolution. In order to take into account the possible damping of axial charge due to gluon topological fluctuations [42], the equation of the net axial current acquires an additional term, which depends on the relaxation time τ_{cs} , so the equation (2) reads:

$$\partial_\mu J_5^\mu = -\frac{n_5}{\tau_{cs}}, \tag{4}$$

where n_5 is the net axial density. The uncertainty in the τ_{cs} is quite large ranging from tenths to hundreds fm [42].

The evolution of the axial density is traced up to freeze-out, which is defined by the condition that the energy density $\text{Ed}=0.18 \text{ GeV}/\text{fm}^3$. Because the effect of the vector meson polarization splitting equally depends on the positive and negative axial charge, at freeze-out the distribution of the absolute value of the axial charge density is obtained.

To calculate the di-lepton invariant mass spectra from the vector mesons emitted from a medium with chiral imbalance, a Monte Carlo model based on the Pythia 8 event generator was used (version 8.2) [44] with a built-in Angantyr collision model for relativistic nuclei [45]. For the simulations, collisions of lead nuclei at an energy of 5.02 TeV were used. In order to increase the statistics of the di-lepton spectrum, the fraction of decays of ρ and ω mesons through the di-electron and di-muon channels was increased up to 0.44.

Decay products were considered in the following rapidity intervals:

$$-0.8 < \eta < 0.8 \text{ for electrons, } -3.6 < \eta < -2.45 \text{ for muons.}$$

This corresponds to the range of the time projection camera and the internal tracking system of the ALICE experiment at the LHC in the central rapidity region

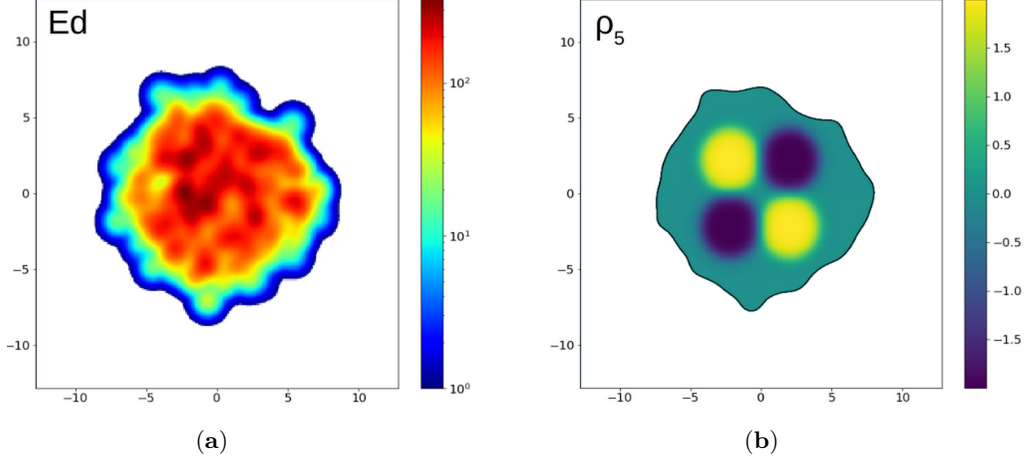


Fig. 1. The initial distribution of energy density (a) and axial charge density (b) in the transverse plane as an example for one Pb-Pb collision event at an energy of 5.02 TeV.

and the muon system in the forward rapidity region [46]. At was initially proposed, to perform the angular analysis in the central rapidity region [13] and ensure the equal treatment of both the di-muon and di-electron channels, for all muon tracks we applied a boost along the z axis by rapidity of 3.05 so that in the new reference frame they lie in the midrapidity. Only di-leptons coming from the decay of light vector mesons were kept for analysis, and background events were not taken into account.

The spectral functions of ρ and ω mesons are shifted in presence of the non-zero chiral charge so that their masses depend on the μ_5 and momentum k as [14]:

$$m_{\rho,\omega}^* = m_{\rho,\omega} + 0.23 \mu_5^2 + 1.37 \mu_5 k + 2.54 \mu_5^2 k^2 \quad (5)$$

(here $m_{\rho,\omega}^*, m_{\rho,\omega}, \mu_5, k$ are in GeV).

Then the leptons momentum is smeared in order to take into account the experimental resolution. The parameters were taken as for the ALICE experiment in the LHC Run 3 conditions (after the LS2 upgrade) [47–49]. The resulting standard deviation of transverse momentum for electrons was taken as 1% and for muons as 0.5%.

Then the di-lepton distributions are calculated with some cuts on the angle θ_A between the leptons [13]. The cuts are selected to keep the reasonable statistics but ensure as good as possible the separate the lepton polarisations.

3. Results

The initial distributions of energy density and axial charge density over the transverse plane are shown in Figure 1 for one example Pb-Pb event.

Then the medium undergo the hydrodynamic evolution. Some intermediate stages are shown in Figure 2. On the 2nd and 3rd panels the snapshots of the axial charge density at the fixed energy density are plotted, which approximately correspond to the fixed proper time τ . The results demonstrate that some smearing is happening and also the neutral area in the center is increasing, however overall the local charge excess stays throughout the entire evolution up to the freeze-out. Due to expansion, the overall scale of the charge density decreases.

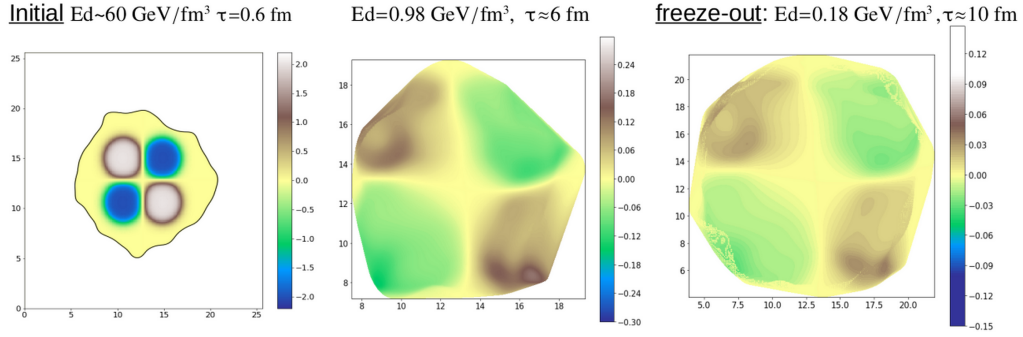


Fig. 2. Hydrodynamic evolution of the axial charge density from initial states to freeze-out, an example for one Pb-Pb collision event at an energy of 5.02 TeV.

Because the effects depend on the absolute value of the axial charge, in Figure 3 we show the distribution of the absolute value of the axial density at the moment of freeze-out, and calculate the mean value $\langle |\rho_5| \rangle$ and standard deviation $\sigma_{|\rho_5|}$ of this distribution.

Then the value of relative fluctuation $\delta_{|\rho_5|} = \sigma_{|\rho_5|} / \langle |\rho_5| \rangle$ is calculated. After the event-by-event study of this value the following result was obtained: $\delta_{|\rho_5|} = 0.42 \pm 0.04$.

Taking into account the estimation of the axial charge density fluctuation we can include it in the calculation of the di-lepton mass distributions. In case of the local thermodynamic equilibrium the axial charge density and axial chemical potential are related, and in the range of our consideration (a few hundreds MeV) the dependence is close to linear. So we put $\delta_{|\rho_5|} \approx \delta_{|\mu_5|}$.

In the Figure 4 the di-electron and di-muon mass distributions are plotted taken into account the fluctuation of the axial chemical potential at the level of 40%, the experimental resolution of ALICE in the Run 3 conditions and the kinematic cuts and selection with angle θ_A between leptons (also shown in the figure). The mean value of axial chemical potential was taken as $\mu_5 = 0.15$ GeV. The results show that the separation of at least two polarisations both for electrons and muons is visible in this conditions.

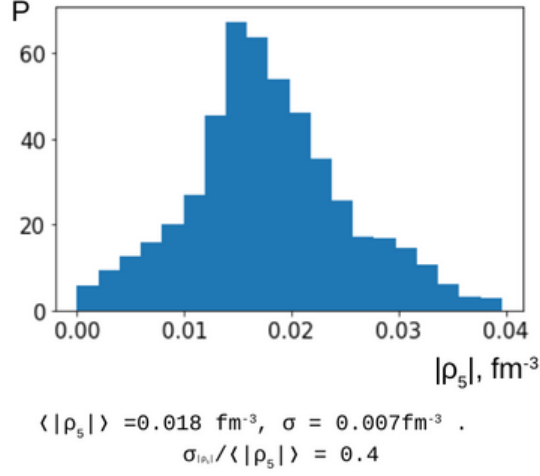


Fig. 3. Distribution of the absolute value of the axial charge density at the freeze-out.

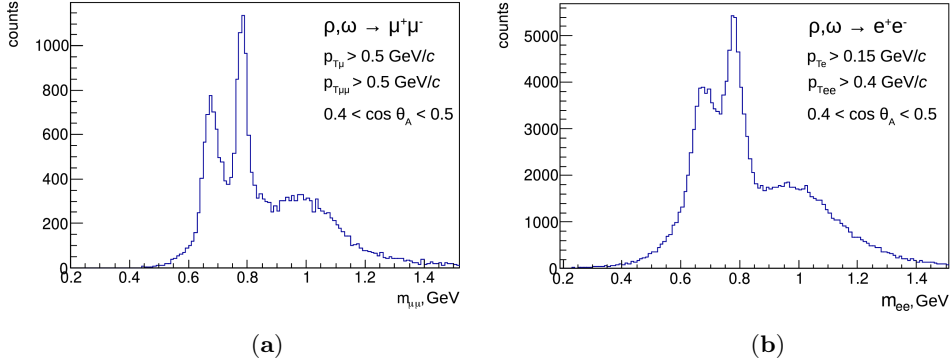


Fig. 4. Invariant mass distribution of di-muons (a) and di-electrons (b) in the Monte Carlo model from the decays of ρ and ω mesons under the expected conditions of the ALICE Run 3 experiment at μ_5 distributed according to Gauss with a mean of 0.15 GeV and a standard deviation $\sigma_{\mu_5} = 0.06$ GeV ($\delta_{\mu} = 40\%$).

4. Dissipative effects

In figure 5 we show for one event, how the results of the axial charge evolution up to freeze-out are modified due to the inclusion of normal viscous effects (diffusion coefficient σ and relaxation time τ_r). We use the values [21, 50] $\sigma = 0.3T$ and $\tau_r = 0.5/T$, where T is the temperature.

We calculated the relative fluctuation $\delta_{|\rho_5|} = \sigma_{|\rho_5|} / \langle |\rho_5| \rangle$ and see that it is increased from 0.39 to 0.44 due to additional smearing caused by viscous effects. However, this increase is quite moderate so it does not affect much the possibility of observing the vector meson polarization splitting.

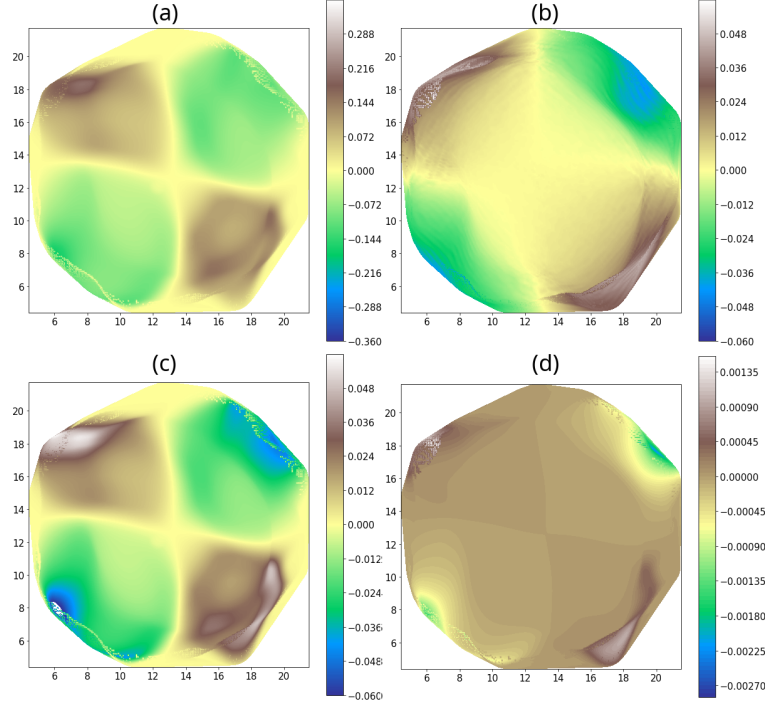


Fig. 5. Modification of freeze-out axial charge distribution: (a) ideal evolution, (b) with viscous effects ($\sigma = 0.3T$ and $\tau_r = 0.5/T$), (c) with axial charge damping ($\alpha_s = 0.2$), (d) with axial charge damping ($\alpha_s = 0.3$).

We also checked the effect of axial charge damping due to gluon topological fluctuations with parameters in the range from $\alpha_s=0.1$, $\tau_{cs} = 113\text{fm}/c$ to $\alpha_s=0.3$, $\tau_{cs} = 1.4\text{fm}/c$ [42] (see table 1). We see that if the Chern-Simons relaxation time is higher than or comparable with the characteristic time of the QGP evolution (up to freeze-out), the distribution of the axial charge survives. However, for small values of τ_{cs} the medium is considerably smoothed out leaving a small chance to observe parity violation effects at the freeze-out.

Table 1. Effect of axial charge damping due to gluon topological fluctuations.

α_s	τ_{cs} (at 300GeV)	$\delta_{ \rho_5 }$
0.1	113 fm/c	0.39
0.2	7.1 fm/c	0.48
0.3	1.4 fm/c	0.80

5. Conclusions

The evolution of the axial chemical potential during the hydrodynamical expansion of the QCD medium, produced in Pb-Pb collisions at LHC energy, has been studied. The results show that the regions of local axial charge excess survive in the medium throughout the entire evolution of the fireball, from the initial stages to freeze-out. The resulting smearing induced by the hydrodynamical evolution is obtained at the level of 40%. The viscous effects moderately increase this variance, leaving the axial charge splitting at a satisfactory level. The effect of gluon topological fluctuations strongly depends on the relaxation time and can smear out the axial charge distribution if τ_{cs} is below the freeze-out time.


The study of the influence of such fluctuation on the possibility of detecting local space parity non-conservation via angular analysis of di-lepton distribution showed that such fluctuations do not destroy the possibility of observing the splitting of vector meson polarizations under the conditions of LHC Run 3 data.

The estimates done in this paper show that a more detailed modeling of initial conditions and the building of a complete framework with parity-violating effects based on EBE-AVFD is deserving. It will allow to study the centrality-dependent effects (including magnetic field) and this can be done in further works.

Acknowledgements

The study was funded by the Russian Science Foundation grant No. 22-22-00493, <https://rscf.ru/en/project/22-22-00493/>

ORCID

Vladimir Kovalenko  <https://orcid.org/0000-0001-6012-6615>

References

1. D. Kharzeev, A. Zhitnitsky, *Charge separation induced by P-odd bubbles in QCD matter*, Nucl. Phys. A **797**, 67 (2007), [arXiv:0706.1026](https://arxiv.org/abs/0706.1026) [hep-ph]
2. K. Buckley, T. Fugleberg, A. Zhitnitsky, *Can theta vacua be created in heavy ion collisions?*, Phys. Rev. Lett. **84**, 4814 (2000), [arXiv:hep-ph/9910229](https://arxiv.org/abs/hep-ph/9910229)
3. D.T. Son, A.R. Zhitnitsky, *Quantum anomalies in dense matter*, Phys. Rev. D **70**, 074018 (2004), [arXiv:hep-ph/0405216](https://arxiv.org/abs/hep-ph/0405216)
4. A.A. Belavin, A.M. Polyakov, A.S. Schwartz, Y.S. Tyupkin, *Pseudoparticle Solutions of the Yang-Mills Equations*, Phys. Lett. B **59**, 85 (1975)
5. L. McLerran, E. Mottola, M.E. Shaposhnikov, *Sphalerons and axion dynamics in high-temperature QCD*, Phys. Rev. D **43**, 2027 (1991)
6. G.D. Moore, K. Rummukainen, *Classical sphaleron rate on fine lattices*, Phys. Rev. D **61**, 105008 (2000), [arXiv:hep-ph/9906259](https://arxiv.org/abs/hep-ph/9906259)
7. E. Shuryak, I. Zahed, *Prompt quark production by exploding sphalerons*, Phys. Rev. D **67**, 014006 (2003), [arXiv:hep-ph/0206022](https://arxiv.org/abs/hep-ph/0206022)
8. D. Kharzeev, R.D. Pisarski, M.H.G. Tytgat, *Possibility of Spontaneous Parity Violation in Hot QCD*, Phys. Rev. Lett. **81**, 512 (1998), [arXiv:hep-ph/9804221](https://arxiv.org/abs/hep-ph/9804221)

9. D. Kharzeev, *Parity violation in hot QCD: Why it can happen, and how to look for it*, Phys. Lett. B **633**, 260 (2006), [arXiv:hep-ph/0406125](#)
10. A.A. Andrianov, V.A. Andrianov, D. Espriu, X. Planells, *Dilepton excess from local parity breaking in baryon matter*, Phys. Lett. B **710**, 230 (2012), [arXiv:1201.3485 \[hep-ph\]](#)
11. A. Andrianov, V.A. Andrianov, D. Espriu, X. Planells, *Abnormal dilepton yield from parity breaking in dense nuclear matter*, AIP Conf. Proc. **1343**, 450 (2011), [arXiv:1012.0744 \[hep-ph\]](#)
12. X. Planells Noguera, A. Andrianov, V. Andrianov, D. Espriu, *QCD effective theories with external chemical potentials*, PoS QFTHEP 2013, 049 (2014)
13. A.A. Andrianov, V.A. Andrianov, D. Espriu, X. Planells, *Analysis of dilepton angular distributions in a parity breaking medium*, Phys. Rev. D **90**, 034024 (2014), [arXiv:1402.2147 \[hep-ph\]](#)
14. V. Kovalenko, A. Andrianov, V. Andrianov, *Vector mesons spectrum in a medium with a chiral imbalance induced by the vacuum of fermions*, J. Phys. Conf. Ser. **1690**, 012097 (2020), [arXiv:2010.13238 \[hep-ph\]](#)
15. D.E. Kharzeev, L.D. McLerran, H.J. Warringa, *The effects of topological charge change in heavy ion collisions: “Event by event P and CP violation”*, Nucl. Phys. A **803**, 227 (2008), [arXiv:0711.0950 \[hep-ph\]](#)
16. G. Wang, *Experimental Overview of the Search for Chiral Effects at RHIC*, J. Phys. Conf. Ser. **779**, 012013 (2017)
17. M.R. Haque, *Measurements of the chiral magnetic effect in Pb–Pb collisions with ALICE*, Nucl. Phys. A **982**, 543 (2019), the 27th International Conference on Ultrarelativistic Nucleus-Nucleus Collisions: Quark Matter 2018, [arXiv:1807.09360 \[hep-ex\]](#)
18. S. Aziz (ALICE), *Search for the Chiral Magnetic Effect with the ALICE detector*, Nucl. Phys. A **1005**, 121817 (2021), [arXiv:2005.06177 \[hep-ex\]](#)
19. X.G. Huang, *Electromagnetic fields and anomalous transports in heavy-ion collisions — A pedagogical review*, Rept. Prog. Phys. **79**, 076302 (2016), [arXiv:1509.04073 \[nucl-th\]](#)
20. Z. Yuan, A. Huang, W.H. Zhou, G.L. Ma, M. Huang, *Evolution of topological charge through chiral anomaly transport*, Phys. Rev. C **109**, L031903 (2024), [arXiv:2310.20194 \[hep-ph\]](#)
21. S. Shi, Y. Jiang, E. Lilleskov, J. Liao, *Anomalous Chiral Transport in Heavy Ion Collisions from Anomalous-Viscous Fluid Dynamics*, Annals Phys. **394**, 50 (2018), [arXiv:1711.02496 \[nucl-th\]](#)
22. S. Shi, H. Zhang, D. Hou, J. Liao, *Signatures of Chiral Magnetic Effect in the Collisions of Isobars*, Phys. Rev. Lett. **125**, 242301 (2020), [arXiv:1910.14010 \[nucl-th\]](#)
23. Y. Jiang, S. Shi, Y. Yin, J. Liao, *Quantifying the chiral magnetic effect from anomalous-viscous fluid dynamics*, Chin. Phys. C **42**, 011001 (2018), [arXiv:1611.04586 \[nucl-th\]](#)
24. D.E. Kharzeev, J. Liao, *Chiral magnetic effect reveals the topology of gauge fields in heavy-ion collisions*, Nature Rev. Phys. **3**, 55 (2021), [arXiv:2102.06623 \[hep-ph\]](#)
25. S. Choudhury et al., *Investigation of experimental observables in search of the chiral magnetic effect in heavy-ion collisions in the STAR experiment*, Chin. Phys. C **46**, 014101 (2022), [arXiv:2105.06044 \[nucl-ex\]](#)
26. W. Li, G. Wang, *Chiral Magnetic Effects in Nuclear Collisions*, Ann. Rev. Nucl. Part. Sci. **70**, 293 (2020), [arXiv:2002.10397 \[nucl-ex\]](#)
27. A. Andrianov, V. Andrianov, D. Espriu, *QCD with Chiral Imbalance: models vs. lattice*, EPJ Web Conf. **137**, 01005 (2017)
28. A.A. Andrianov, V.A. Andrianov, D. Espriu, A.E. Putilova, A.V. Iakubovich, *Decays*

- of light mesons triggered by chiral chemical potential, *Acta Phys. Polon. Supp.* **10**, 977 (2017), [arXiv:1707.06150 \[hep-ph\]](#)
29. A.A. Andrianov, V.A. Andrianov, D. Espriu, A.V. Iakubovich, A.E. Putilova, *QCD with Chiral Chemical Vector: Models Versus Lattices*, *Phys. Part. Nucl. Lett.* **15**, 357 (2018)
 30. A. Andrianov, V. Andrianov, D. Espriu, *Chiral Perturbation Theory vs. Linear Sigma Model in a Chiral Imbalance Medium*, *Particles* **3**, 15–22 (2020)
 31. V.N. Kovalenko, V.V. Petrov, *The possibility of finding the p symmetry breaking decay of the charged a_0 meson*, *Bull. Russ. Acad. Sc. Phys.* **88**, 1327–1331 (2024)
 32. V.V. Petrov, V.N. Kovalenko, *The Possibilities of Search for the Local Strong P -Symmetry Breaking in Decay of Charged a_0 Meson in $3\pi^\pm$ Decay Channel*, *Phys. Part. Nucl.* **55**, 1005–1009 (2024)
 33. Putilova, A.E., Iakubovich, A.V., Andrianov, A.A., Andrianov, V.A., Espriu, D., *Exotic meson decays and polarization asymmetry in hadron environment with chiral imbalance*, *EPJ Web Conf.* **191**, 05014 (2018)
 34. B. Schenke, S. Jeon, C. Gale, *(3+1)D hydrodynamic simulation of relativistic heavy-ion collisions*, *Phys. Rev. C* **82**, 014903 (2010), [arXiv:1004.1408 \[hep-ph\]](#)
 35. B. Schenke, S. Jeon, C. Gale, *Higher flow harmonics from (3+1)D event-by-event viscous hydrodynamics*, *Phys. Rev. C* **85**, 024901 (2012), [arXiv:1109.6289 \[hep-ph\]](#)
 36. J.F. Paquet, C. Shen, G.S. Denicol, M. Luzum, B. Schenke, S. Jeon, C. Gale, *Production of photons in relativistic heavy-ion collisions*, *Phys. Rev. C* **93**, 044906 (2016), [arXiv:1509.06738 \[hep-ph\]](#)
 37. J.F. Paquet, *Simulating heavy ion collisions with MUSIC*, Available online: https://webhome.phy.duke.edu/~jp401/music_manual/ (Accessed on 29.01.2023)
 38. C. Shen, *SuperMC, Monte Carlo event generator of initial density distributions for relativistic heavy-ion collisions*, Available online: <https://github.com/chunshen1987/superMC> (Accessed on 29.01.2023)
 39. C. Shen, Z. Qiu, H. Song, J. Bernhard, S. Bass, U. Heinz, *The iEBE-VISHNU code package for relativistic heavy-ion collisions*, *Comput. Phys. Commun.* **199**, 61 (2016), [arXiv:1409.8164 \[nucl-th\]](#)
 40. T.D. Lee, G.C. Wick, *Vacuum Stability and Vacuum Excitation in a Spin 0 Field Theory*, *Phys. Rev. D* **9**, 2291 (1974)
 41. D. Kharzeev, A. Zhitnitsky, *Charge separation induced by P -odd bubbles in QCD matter*, *Nucl. Phys. A* **797**, 67 (2007), [arXiv:0706.1026 \[hep-ph\]](#)
 42. A. Huang, S. Shi, S. Lin, X. Guo, J. Liao, *Accessing topological fluctuations of gauge fields with the chiral magnetic effect*, *Phys. Rev. D* **107**, 034012 (2023), [arXiv:2106.10847 \[hep-ph\]](#)
 43. J. Lömker, *AVFD_Node*, Available online: https://github.com/jloemker/EbE_AVFD_1p2-LHC/tree/main/AVFD_Node/AVFDTransport (2022) (Accessed on 22.07.2024)
 44. T. Sjöstrand, S. Ask, J.R. Christiansen, R. Corke, N. Desai, P. Ilten, S. Mrenna, S. Prestel, C.O. Rasmussen, P.Z. Skands, *An introduction to PYTHIA 8.2*, *Comput. Phys. Commun.* **191**, 159 (2015), [arXiv:1410.3012 \[hep-ph\]](#)
 45. C. Bierlich, G. Gustafson, L. Lönnblad, H. Shah, *The Angantyr model for Heavy-Ion Collisions in PYTHIA8*, *JHEP* **10**, 134 (2018), [arXiv:1806.10820 \[hep-ph\]](#)
 46. Aamodt K. et al (ALICE Collaboration), *The ALICE experiment at the CERN LHC*, *JINST* **3**, S08002 (2008)
 47. Abelev B. et al (ALICE Collaboration), *Technical Design Report for the Upgrade of the ALICE Inner Tracking System*, *J. Phys. G* **41**, 087002 (2014)
 48. E. Garcia-Solis (ALICE Collaboration), *Perspectives of the ALICE Experiment and Detector Upgrade*, *Nucl. Part. Phys. Proc.* **267-269**, 382 (2015)

49. Adam J. et al (ALICE Collaboration), *Technical Design Report for the Muon Forward Tracker*, Tech. rep. CERN-LHCC-2015-001, ALICE-TDR-018, 2015
50. G.S. Denicol, H. Niemi, I. Bouras, E. Molnar, Z. Xu, D.H. Rischke, C. Greiner, *Solving the heat-flow problem with transient relativistic fluid dynamics*, Phys. Rev. D **89**, 074005 (2014), [arXiv:1207.6811 \[nucl-th\]](#)